Research Article

Quasi-Dimensional Modelling and Parametric Studies of a Heavy-Duty HCCI Engine

Sunil Kumar Pandey,[1] Muralitharan N.,[1] and Ravikrishna R. V.[2]

[1] Engine Research and Development, Ashok Leyland., Hosur, Tamil Nadu 635129, India
[2] Combustion and Spray Laboratory, Department of Mechanical Engineering, Indian Institute of Science, Bangalore, Karnataka 560012, India

Correspondence should be addressed to R. V. Ravikrishna, ravikris@mecheng.iisc.ernet.in

A quasi-dimensional modelling study is conducted for the first time for a heavy duty, diesel-fuelled, multicylinder engine operating in HCCI mode. This quasidimensional approach involves a zero-dimensional single-zone homogeneous charge compression ignition (HCCI) combustion model along with a one-dimensional treatment of the intake and exhaust systems. A skeletal chemical kinetic scheme for n-heptane was used in the simulations. Exhaust gas recirculation (EGR) and compression ratio (CR) were the two parameters that were altered in order to deal with the challenges of combustion phasing control and operating load range extension. Results from the HCCI mode simulations show good potential when compared to conventional diesel performance with respect to important performance parameters such as peak firing pressure, specific fuel consumption, peak pressure rise, and combustion noise. This study shows that HCCI combustion mode can be employed at part load of 25% varying the EGR rates between 0 and 60%.

1. Introduction

HCCI mode of operation has the potential to significantly reduce NO_x and particulate emissions, while achieving high thermal efficiency and having the capability of operating with a variety of fuels. To a degree, the HCCI combustion process is able to combine the best features of a Spark Ignition (SI) engine using gasoline fuel and a Compression Ignition (CI) engine using diesel fuel. Similar to an SI engine, the fuel and air are mixed to obtain a homogeneous mixture, which can eliminate fuel-rich diffusion combustion and can thus dramatically reduce the particulate emissions that are usually associated with conventional diesel combustion processes. Current research efforts are focused mainly towards finding solutions to challenges of combustion phasing control, operating load range extension, unburned hydrocarbon (HC) and carbon monoxide (CO) emissions reduction. One-dimensional simulation studies combined with realistic chemical mechanisms have proven to be a reliable method of exploring these challenges. Nonavailability of chemical kinetic mechanisms for realistic fuels like gasoline and diesel can be compensated by using standard reference fuels like n-heptane, n-butane, and isooctane. These fuels are considered to be covering an appropriate range of ignition behaviour typical for higher hydrocarbons. Of these, n-heptane shows ignition properties closer to those of diesel. Generally, chemical kinetics calculations with the detailed mechanisms for time-varying compression and expansion can be conducted to understand the ignition behavior of different cases across the expected operating range [1].

Several modelling strategies have been used to study HCCI operation in engines. For the combustion chamber, both single-zone and multizone approaches have been applied previously [2, 3]. The single-zone or multizone model requires initial conditions to be specified at intake valve closing (IVC), including the average temperature, pressure of the mixture, and each concentration of species in the cylinder. These initial conditions are difficult to be

TABLE 1: Engine specification.

Engine configuration	4 cylinder, in-line
Bore × stroke (mm)	112 × 135
Fuel system	1800 bar, common rail
Compression ratio (-)	17.5 : 1
Scavenging system	TCIC
Rated power (kW)	140
Maximum torque (Nm)	700

obtained in a test engine. Considering the importance of these initial conditions for simulation accuracy, the one-dimensional HCCI engine cycle model combining both detailed combustion chemistry and gas exchange processes needs to be developed so that the initial conditions at IVC no longer have to be specified. The gas exchange process affects the engine parameters and charge properties and, therefore, plays a significant role in determining the control of the HCCI process. Therefore, the one-dimensional modelling is useful to analyze the influence of the variable valve timing strategy on the gas exchange. Generally, the one-dimensional model is constructed by combining CHEMKIN code package and a one-dimensional engine simulation tool. The single-zone HCCI combustion model assumes that the combustion chamber is a well-stirred reactor with a uniform temperature, pressure, and composition. This model is applicable to homogeneous charge engines, where mixing is not a controlling factor. Single-zone analyses can predict start of combustion with good accuracy if the conditions at the beginning of the compression stroke are known and, therefore, can be used to explore ranges of operation for different fuels and conditions.

In the multizone approach, the cylinder is divided into zones and thermal boundary layer, providing a more realistic distribution of the charge temperature and concentration.

Wang et al. [4] studied the detailed chemical kinetics of HCCI by implementing it into each of the zero-dimensional, single-zone model, one-dimensional engine cycle model, and three-dimensional CFD model. They carried out simulation and experiment on a four-stroke gasoline HCCI engine with direct injection. Ryan III and callahan . [5] examined the effect of variables like air-fuel ratio, compression ratio, fresh intake air temperature, EGR, and intake mixture temperatures on HCCI knock and misfire. They demonstrated that acceptable HCCI combustion was achieved if ignition occurred within approximately 20 degrees of top dead center (TDC). If ignition was delayed until after TDC, the combustion was unacceptable and generally resulted in significant misfire. The misfire frequency increased as the temperature in the combustion chamber dropped due to poor combustion. The initial experiments also indicated that HCCI was most dependent on the EGR rate, followed by the compression ratio and the air-fuel ratio.

The motivation of this work is derived from the fact that HCCI combustion mode can be gainfully employed at part load and the conventional diesel combustion mode can be used for higher load conditions. Such a dual-mode operation can be very beneficial in intracity bus applications, where the major part of operation occurs at intermediate speed and load ranges. Also, a quasi-dimensional approach towards simulating heavy-duty, diesel-fuelled HCCI operation is not found in the literature. Based on this motivation, an engine currently in use for intracity bus application in India was chosen. The chosen engine configuration is shown in Table 1.

Figure 1 shows the measured duty cycle of the engine under consideration. The total trip time during the study was 45 minutes. The major part of the operation of the engine was between 850 and 1450 rpm and in the load range of 35–78%. Significant operation was also seen in the 20–35% load range.

Based on the above measurement data, it was decided to carry out the simulation study for HCCI mode in the range of 900–1700 rpm in the load range of 25–75%. The present study focuses on simulating the engine system with a one-dimensional commercial code AVL Boost v10, using the single-zone HCCI combustion model. A skeletal n-heptane chemical kinetic scheme [6] is used for the calculations. The fuel injection is modelled in order to simulate early direction injection. The effect of EGR on combustion phasing is explored in this study for the operating condition of 1400 rpm and 25% load.

2. Modeling Methodology

2.1. Modeling of the Gas Exchange Process. The intake and exhaust processes are treated as one-dimensional. The pressures, temperatures, and flow velocities obtained from the solution of the gas dynamic equations represent mean values over the cross-section of the pipes. The governing equations for the one-dimensional flow in the intake and exhaust runners are given below. The one-dimensional pipe flow is described by the Euler equation:

$$\frac{\partial U}{\partial t} + \frac{\partial F(U)}{\partial x} = S(U), \tag{1}$$

where U represents the state vector and F is the flux vector. The source term on the right-hand side comprises two different source terms:

$$S(U) = S_A(F(U)) + S_R(U), \tag{2}$$

where S_A is the source caused by axial changes in the pipe cross-section and S_R is the source taking into account homogeneous chemical reactions, heat and mass transfer terms between the gas and solid phase, and friction sources. The details can be found elsewhere [7, 8].

2.2. Single-Zone HCCI Combustion Model. The details of the single-zone HCCI combustion model are briefly mentioned in Section 2.3; however, the details can be found elsewhere [7]. The first law of thermodynamics gives the state of the cylinder as follows in a general form:

$$\frac{d(m_c \cdot u)}{d\alpha} = -p_c \cdot \frac{dV}{d\alpha} + \frac{dQ_F}{d\alpha} - \Sigma \frac{dQ_w}{d\alpha} - h_{BB} \cdot \frac{dm_{BB}}{d\alpha} \\ + \Sigma \frac{dm_i}{d\alpha} \cdot h_i - \Sigma \frac{dm_e}{d\alpha} \cdot h_e - q_{ev} \cdot f \cdot \frac{dm_{ev}}{dt}. \tag{3}$$
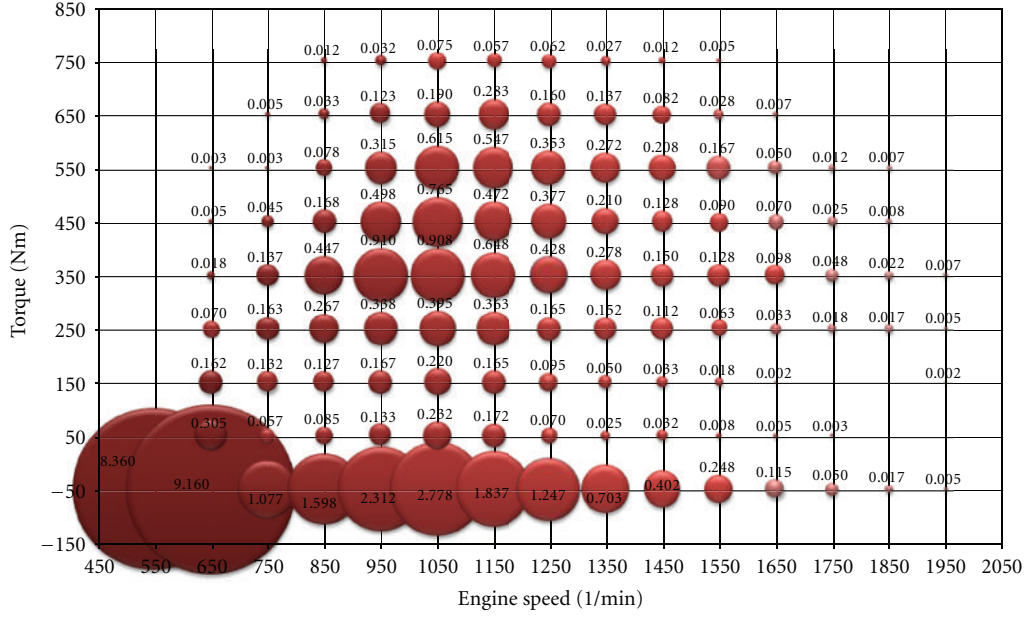
FIGURE 1: Duty cycle of chosen engine on an intracity bus application.

The variation of mass in cylinder is calculated as

$$\frac{dm_c}{d\alpha} = \Sigma \frac{dm_i}{d\alpha} - \Sigma \frac{dm_e}{d\alpha} - \frac{dm_{BB}}{d\alpha} + \frac{dm_{ev}}{dt}, \quad (4)$$

where subscripts c, i, and e denote the cylinder, inflow, and outflow conditions, respectively, u is the specific internal energy, p_c is the cylinder pressure, V is the cylinder volume, Q_F is the fuel energy, Q_w is the wall heat loss, h_{BB} and m_{BB} are the enthalpy and mass flow of the blow-by, respectively, q_{ev} is the evaporation heat of the fuel, f is the fraction of evaporation heat from the cylinder charge, m_{ev} is the mass of evaporating fuel, and α is the crank angle.

For single-zone HCCI, the fuel heat input is formulated as

$$\frac{dQ_F}{d\alpha} = \sum_{i=1}^{nSpcGas} u_i \cdot MW_i \cdot \dot{\omega}_i. \quad (5)$$

The species mass fractions are calculated as

$$\rho \frac{dw_i}{d\alpha} = MW_i \cdot \dot{\omega}_i, \quad (6)$$

where subscript i is used for individual species, $nSpcGas$ is the number of species, u_i is the species internal energy, MW_i is the species molecular weight, ρ is the mixture density, w_i is the species mass fraction, and $\dot{\omega}_i$ is the species reaction rate.

The reaction rate of each species is calculated based on a set of chemical reactions.

2.3. Engine Simulation Model.
The first step in our study was to validate the engine simulation model with respect to experimental results in the conventional compression ignition diesel mode. The simulation model was then modified for HCCI mode. The purpose of comparing the

conventional CI engine model predictions with experimental data was to validate the various aspects of the engine such as intake and exhaust processes, and their coupling with the in-cylinder zero-dimensional combustion model. Once this was done, it was possible to replace the conventional combustion model with an appropriate model suitable for HCCI combustion.

2.3.1. Conventional Compression Ignition Engine Model.
Figure 2 shows the engine model created in AVL BOOST v10 for the engine simulation. The air enters into the aircleaner CL1 through the system boundary SB1. The air then gets compressed in the compressor C of turbocharger TC1 and goes to the intake manifold PL1 via air cooler CO1. After combustion, the exhaust gas enters the turbine T of the turbocharger TC1. A catalytic converter CAT1 and a plenum chamber PL2 are connected for maintaining backpressure after the turbine T. EGR supply to the intake manifold is taken from Junction $J4$ which forms a part of the exhaust manifold. The EGR rate is controlled using a PID controller. MP1 to MP9 are the points where the thermodynamic properties are monitored. The details of the heat transfer model for the ports and the liners can be found elsewhere [7].

Two common methods to simulate a direct injection compression ignition engine that are available in AVL Boost are the Mixing Controlled Combustion (MCC) model and the Predefined Heat Release model [7, 8]. The MCC model is the one where the model considers the effects of the premixed and diffusion-controlled combustion process. The Predefined Heat Release model includes
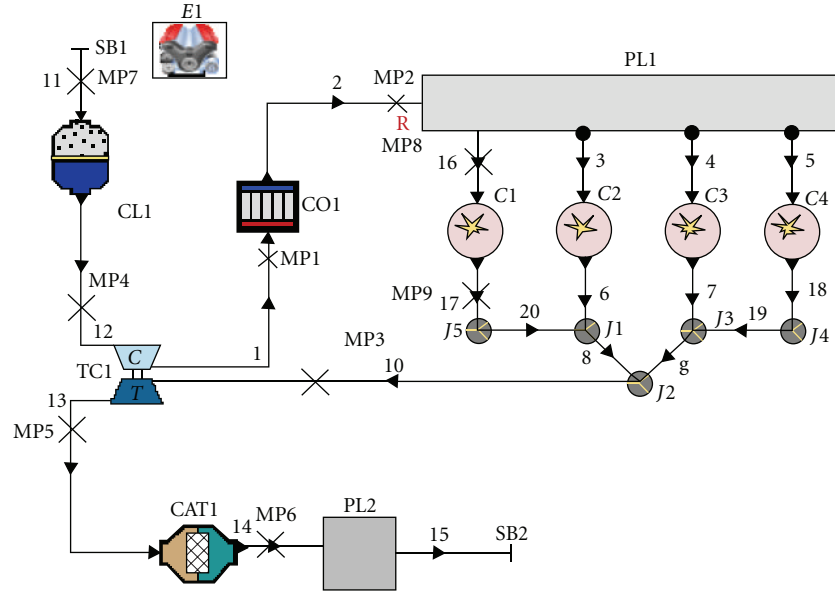
(a) Vibe and Table,

(b) Extended heat release.

FIGURE 2: Simulation model of engine system.

While the Extended heat release model is used for transient calculations, the Vibe function is used to approximate the actual heat release characteristics of an engine. The "Table method" is a simple approach of modelling combustion process by the direct specification of the rate of heat release of equivalent engines from the benchmark data. This rate of heat release together with the amount of fuel in the cylinder and *A/F* ratio is used to calculate the heat input per degree of crank angle. The Table method is used to model the combustion for the conventional CI combustion process in this study. The rate of heat release from an equivalent engine available from benchmark data is used as an input.

2.3.2. HCCI Engine Model. The combustion model of the engine simulation model shown in Figure 2 is replaced with zero dimensional single-zone HCCI. This model implemented in AVL Boost is also incorporated in AVL FIRE and is called stand-alone 0D reactor model which is used to carry out 0D calculations, details of which can be found elsewhere [9]. This is a simplification of the single-zone 0D reactor model which is used in order to account for the effect of chemistry. In the stand-alone 0D reactor model, the volume of the 0D reactor is a function of time according to

$$\frac{V(t)}{V} = 1 + \frac{C-1}{2}\left[R + 1 - \cos\alpha - \sqrt{R^2 - \mathrm{Sin}^2\,\alpha} \right], \quad (7)$$

where V is the volume of the cylinder, C is the compression ratio, R is the ratio of the crank radius to connecting rod length, and α is the crank angle. The single-zone HCCI/stand-alone 0D reactor model has been validated extensively in the literature [10–12]. The n-heptane skeletal mechanism developed by Raya [6] incorporating 24 species and 63 reactions is used which is validated for HCCI applications in their work. The EGR is supplied at the inlet

boundary for theoretical study. In-cylinder fuel vaporization is specified in order to simulate direct injection.

3. Results and Discussions

The parameters considered for conventional compression ignition engine validation are heat release rate, in-cylinder pressure, specific fuel consumption, peak firing pressure, boost pressure, fuel flow, air flow, and combustion noise. The parameters considered for the study of HCCI engine are heat release rate, in-cylinder pressures and temperatures, peak pressure rise, combustion noise, EGR rate, and compression ratio variation. These results are discussed in Section 3.1.

3.1. Validation of Engine Model in Conventional Compression Ignition Mode. Figure 3 shows the comparison of experimental versus simulated heat release rate for the rated operating point. The experimental maximum value of heat release rate is 200 J/deg, while the simulation maximum value is 184.6 J/deg. Overall, the agreement is reasonably good. The effect of post-injection is not visible in simulation results as the chosen combustion model does not take the pilot and post-injection into account.

Figure 4 shows the comparison of experimental versus simulated in-cylinder pressure for the rated operating point. Here again, it is observed that the comparison is favourable, with a difference of around 9% at the peak value.

Figures 5, 6, 7, 8, 9, and 10 show the comparison of experimental and simulated values for normalized specific fuel consumption, peak firing pressure, boost pressure, normalized fuel flow, air flow, and combustion noise, respectively, for the full range of engine speeds in full throttle condition. In Figure 6, the drop in peak firing pressure at 1300 rpm is
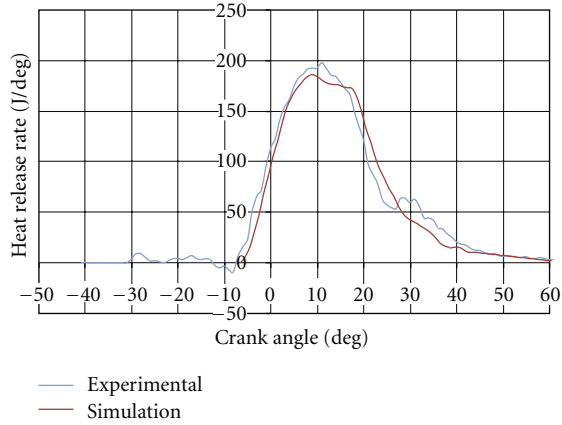
FIGURE 3: Comparison of experimental and simulated values of heat release rate (2300 rpm; 100% load).
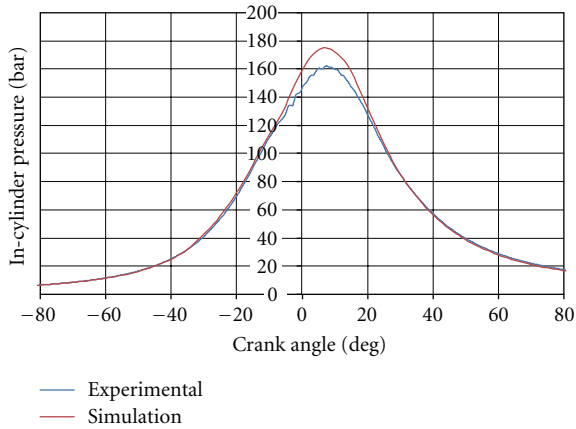

FIGURE 4: Comparison of experimental and simulated values of in-cylinder pressure (2300 rpm; 100% load).
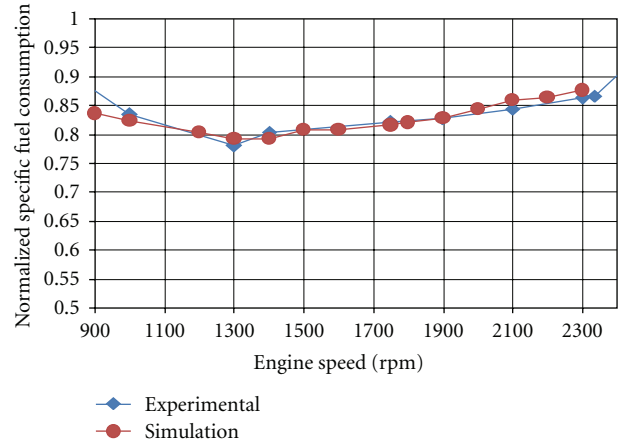

FIGURE 5: Comparison of experimental and simulated values of normalized specific fuel consumption.
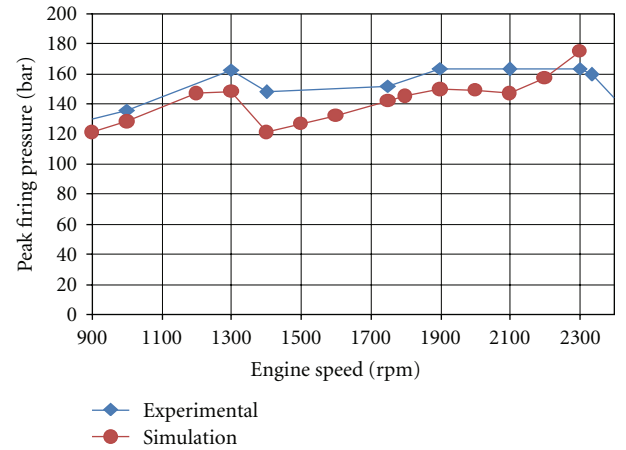
FIGURE 6: Comparison of experimental and simulated values of peak firing pressure.

due to start of EGR from this point onwards. In the case of experiments, the combustion noise is calculated from the measured cylinder pressure trace using AVL Concerto [13]. The simulated combustion noise is calculated by AVL Boost from the calculated cylinder pressure trace. Overall, it can be observed that the engine model predictions match very well with experimental data for the conventional CI mode. This implies that certain aspects of the model such as the intake and exhaust processes and their coupling with the in-cylinder conditions are wellvalidated. Thus, this engine model in conjunction with the single-zone HCCI model which has been validated in the literature serves as an effective tool to explore engine performance in the HCCI mode.

3.2. HCCI Engine Model

3.2.1. Description of Heat Release Rate. Next, the engine operation in the HCCI mode is considered utilizing the single-zone model described earlier. **Figure 11** shows the heat release rate for the 25% load condition of 1400 rpm

using the skeletal n-heptane chemistry of Raya [6]. From **Figure 11**, it is observed that there is a two-stage heat release. This is in agreement with previous studies wherein a similar heat release profile has been reported [1]. The first stage of the heat release curve is associated with low-temperature kinetic reactions, and the time delay between the first and main heat releases is because of "Negative Temperature Coefficient (NTC) regime" which lies between the two stages of heat release. According to Yao et al. [1], there are three combustion regimes of hydrocarbon fuels. After removal of an H atom from the n-heptane fuel molecule, the heptyl radical can react with molecular oxygen to form an alkylperoxy radical. The low-temperature path continues with an isomerization step, and a hydroperoxy alkyl radical is formed due to transformation of this alkylperoxy radical. A second oxygen molecule is added to the product of the isomerization step, and the oxohydroperoxide radical can then isomerise further and decompose into a relatively stable ketohydroperoxide species and OH radicals. With further increase in temperature, the alkylperoxy radicals
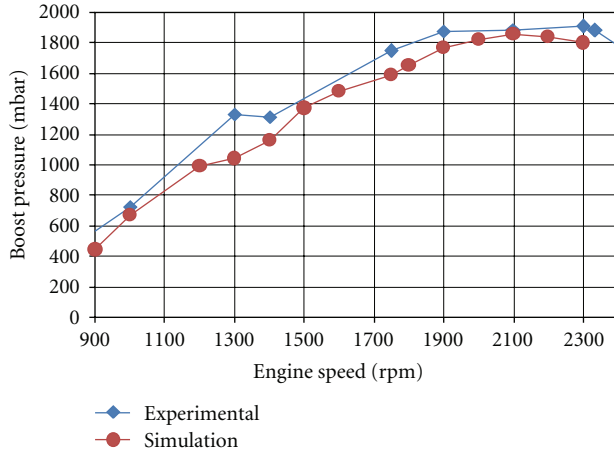
FIGURE 7: Comparison of experimental and simulated values of boost pressure.
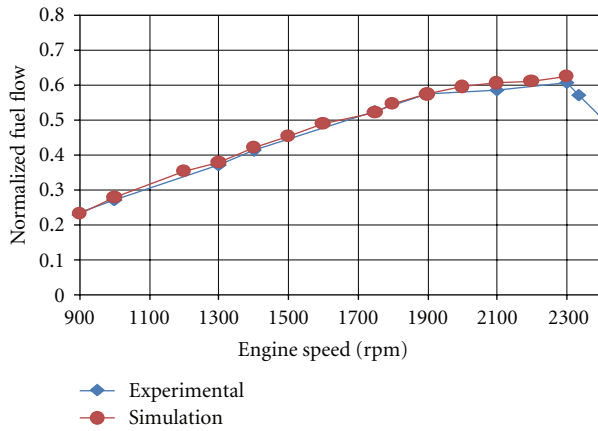

FIGURE 9: Comparison of experimental and simulated values of air flow.

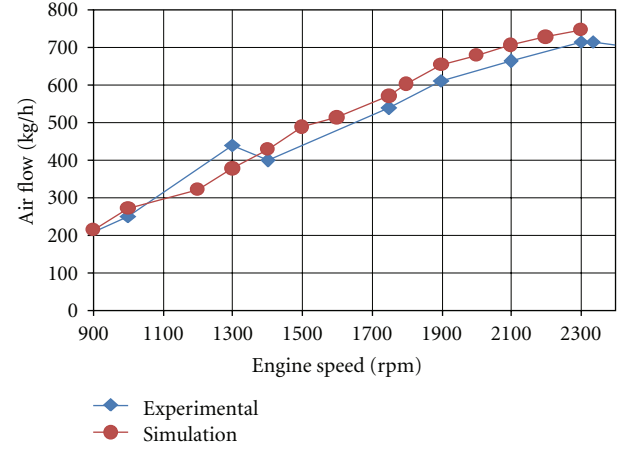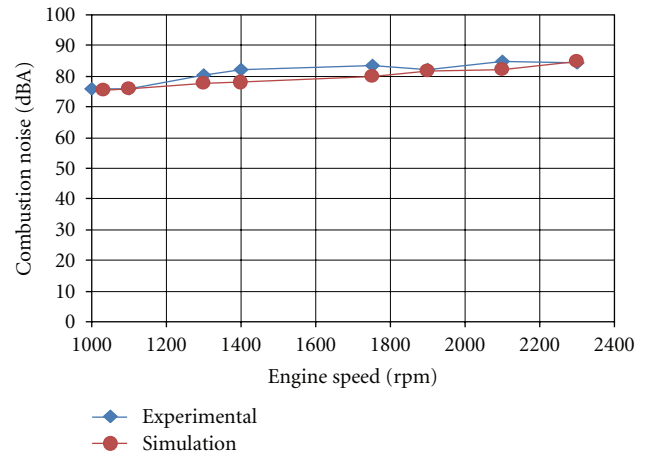FIGURE 8: Comparison of experimental and simulated values of normalized fuel flow.

FIGURE 10: Comparison of experimental and simulated values of combustion noise.

decompose back into initial reactants. The formation of olefins and hydroperoxyl radicals is favoured, and the overall reaction rate decreases with the increase of temperature. This NTC behaviour is observed in low-temperature oxidation of paraffinic fuels. In the high-temperature regime, the increasing temperature is high enough, and the hydrogen-oxygen branching reactions control the reaction rate. The heat release rate of this stage is dominated by the oxidation process of carbon monoxide to carbon dioxide.

Noguchi et al. [14] had done spectroscopic measurements showing that CH_2O, HO_2, and O radical concentrations are high before autoignition. These species are characteristic of low-temperature autoignition chemistry of larger paraffinic hydrocarbon fuels. After first stage of ignition, the CH, H, and OH radicals are high in concentration, which indicate high-temperature chemistry during the bulk burn. Figures 12, 13, 14, and 15 show the CH_2O/HO_2, O, OH, and H radical formations, respectively. It can be observed that CH_2O and HO_2 radicals are high before 345 deg CA which is the start of autoignition and OH and H radicals are

high after the start of autoignition. The O radical formation starts towards the end of autoignition, which needs to be investigated further.

3.2.2. Effect of EGR Rate on Combustion Phasing. Figure 16 shows the effect of varying EGR rate from 0% to 60% on the heat release rate. The first stage of combustion diminishes with increasing EGR rate. The second stage of combustion increases with increasing EGR rate till 40% EGR, and then it drops. The NTC regime is seen to expand as the EGR rate is increased. Table 2 shows the location of 5%, 50%, and 90% mass burned fraction (MBF) for different EGR rates. It can be observed from the crank angle values corresponding to the MBF of 50% that the retardation of combustion is approximately 4-5 degrees with a 20% increase in the EGR rate. Figure 17 shows the variation of MBF versus the crank angle for 0%, 20%, 40%, and 60% EGR rates.

Figures 18 and 19 show the effect of varying EGR rate from 0% to 60% on the in-cylinder pressure and temperature. The peak value remains constant for 0%, 20%,
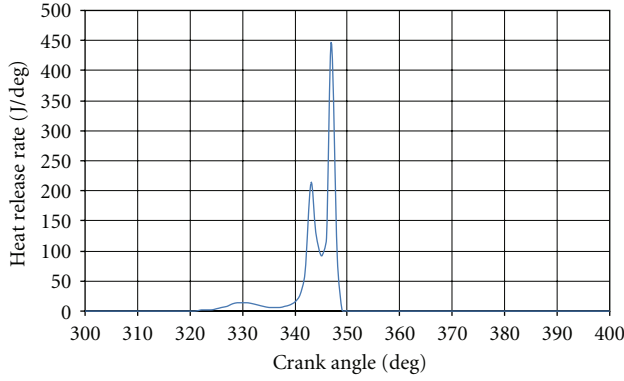
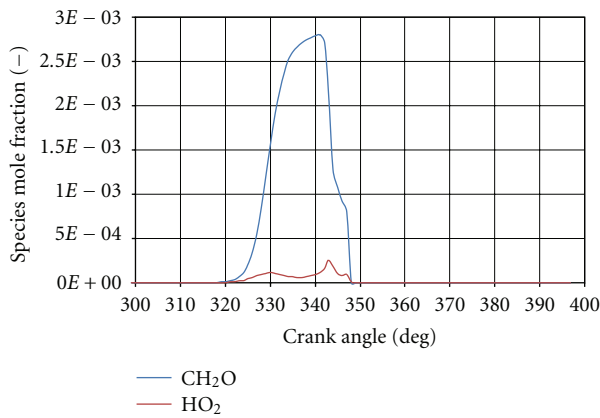FIGURE 11: Heat release rate (1400 rpm; 25% load; 17.5 CR, 0% EGR).

FIGURE 12: CH_2O and HO_2 radical formation (1400 rpm; 25% load; 17.5 CR; 0% EGR).

FIGURE 13: O radical formation (1400 rpm; 25% load; 17.5 CR; 0% EGR).
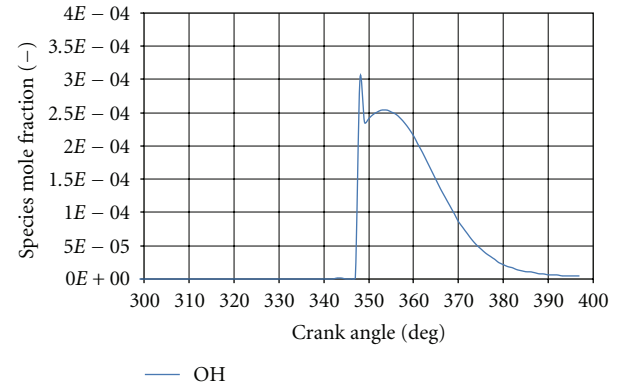
FIGURE 14: OH radical formation (1400 rpm; 25% load; 17.5 CR; 0% EGR).

TABLE 2: Location of 5%, 50%, and 90% mass burned fraction in degree CA for 0%, 20%, 40%, and 60% EGR rates.

MBF	EGR rates			
	0%	20%	40%	60%
5%	−25.8	−16.0	−10.6	−8.7
50%	−13.4	−9.5	−4.3	0.2
90%	−11.7	−7.7	−2.2	3.7

and 40% EGR rates. A drop of 9 bar is seen in the case of 60% EGR. The maximum in-cylinder temperature seen is 1920 K for 0% EGR rate and drops to 1780 K with 60% EGR rate.

3.2.3. Effect of Compression Ratio on Peak Firing Pressure. Figure 20 shows the effect of compression ratio on in-cylinder pressure for the cases of 17.5, 16.5, and 15.5. A reduction of compression ratio from 17.5 to 15.5 shows the potential of reducing the peak firing pressure by 18 bar.

3.2.4. Part Load Potential of HCCI Operation. Table 3 shows the effect of variation of EGR rate from 0% to 60% on the performance parameters for the case of 1400 rpm and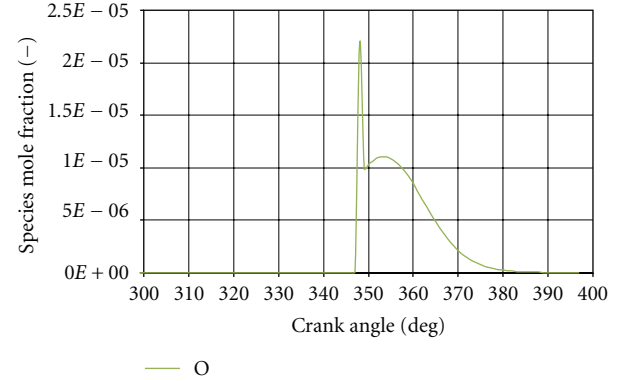 25% load case. The result is also compared with the experimental values of the conventional CI mode. For the 1400 rpm and 25% load case, 60% EGR rate with HCCI operation gives better SFC than conventional CI mode. Also, the HCCI operation shows acceptable peak firing pressure, marginally high combustion noise and acceptable peak pressure rise. The maximum peak pressure rise observed in case of conventional CI mode is 5.8 bar/deg in the full throttle condition. Typically, in the HCCI mode, higher peak pressure rise values are observed. In 0% EGR condition, the maximum peak pressure rise observed was 37.2 bar/deg. However, the peak pressure rise reduces with increase in EGR rate and drops to the level of 9.2 bar/deg for 60% EGR rate which is acceptable.

4. Conclusions

In the present paper, quasi-dimensional simulations of HCCI operation for a heavy-duty, diesel-fuelled engine have been reported for the first time to the best of our knowledge. A zero-dimensional, single-zone model is used for the combustion chamber using a skeletal n-heptane chemical kinetic scheme. The following conclusions can be drawn.

TABLE 3: Performance parameters of HCCI mode simulation results with varying EGR condition and comparison with CI mode experimental values (Operating condition: 1400 rpm; 25% load; compression ratio:17.5; fuel quantity: 38.5 mg/stroke).

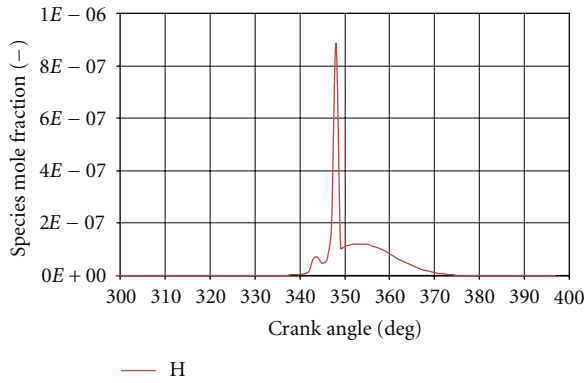| Mode	HCCI	HCCI	HCCI	HCCI	CI
EGR rate	0%	20%	40%	60%	20%
Power (kW)	19.4	23.44	27.6	29.4	24.6
Peak firing pressure (bar)	124.7	123.8	126.1	117.4	65.6
Peak pressure rise (bar/deg)	37.2	33.7	23.8	9.2	3.2
Combustion noise (dBA)	98.9	99.0	96.7	91.5	83.8
Specific fuel consumption (g/kW-h)	332.7	275.5	233.6	219.2	242.1

FIGURE 15: H radical formation (1400 rpm; 25% load; 17.5 CR; 0% EGR).

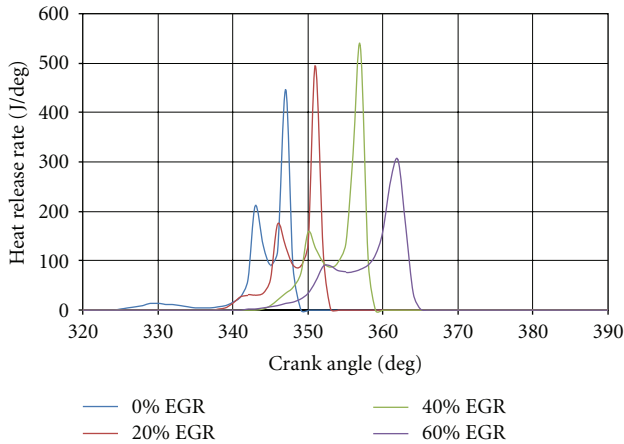FIGURE 17: Effect of EGR on mass burned fraction (1400 rpm; 25% load; 17.5 CR).

FIGURE 16: Effect of EGR on heat release rate (1400 rpm; 25% load; 17.5 CR).

(i) The two-stage heat release rate is clearly observed in this study which is typical for diesel-like fuels in HCCI mode.

(ii) The effect of adding EGR is to reduce the magnitude of the first stage of heat release. The NTC regime is observed to widen with increased EGR rates.

(iii) Higher EGR rates tend to give improved SFC due to shift of the pressure diagram towards the TDC. The combustion gets retarded by 4-5 degree crank angle for every 20% EGR rate increase for the 25% load case.
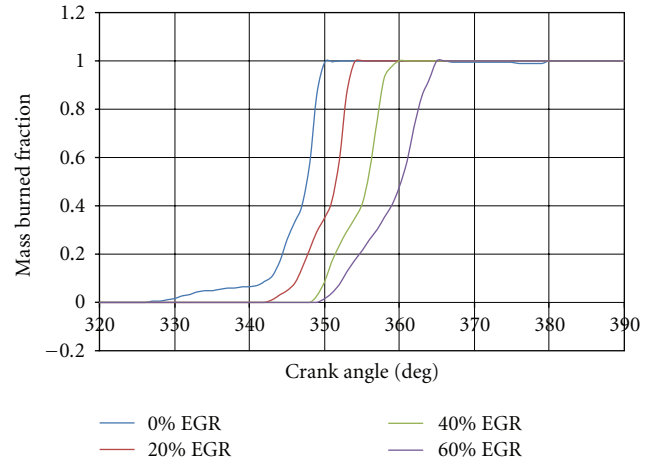
(iv) EGR rate as high as 40–60% was observed to produce near acceptable values of specific fuel consumption, peak firing pressure, and combustion noise. However, the peak pressure rise was found to be between 9 and 38 bar/deg in the investigated operating conditions.

(v) Parametric study of compression ratio showed that reduction of compression ratio from 17.5 to 15.5 has the potential to reduce the peak firing pressure by 18 bar.

(vi) Overall, the study shows that the current engine configuration has the potential to operate satisfactorily in the HCCI mode at 25% load. This study has helped to identify a range of engine parameters for which HCCI performance is observed to be superior compared to the conventional CI mode.

Future efforts will focus on reducing the peak pressure rise further and conducting three-dimensional simulations for the engine configuration identified in this study.
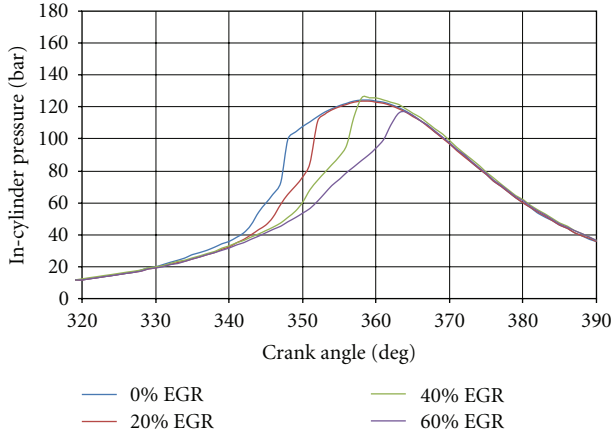
Figure 18: Effect of EGR on in-cylinder pressure (1400 rpm; 25% load; 17.5 CR).
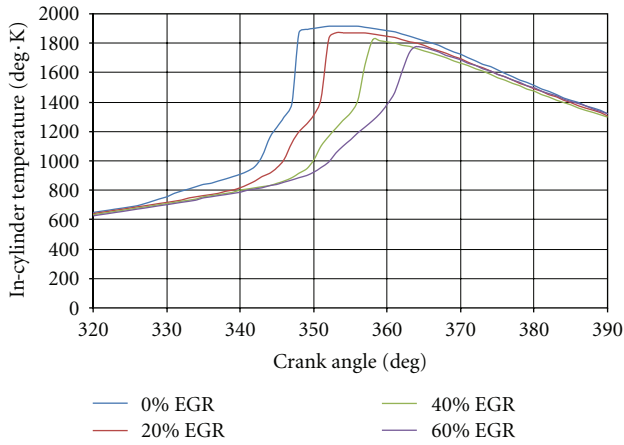

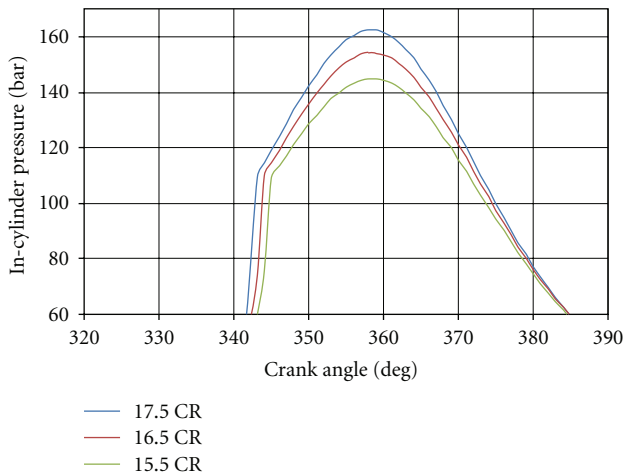Figure 19: Effect of EGR on in-cylinder temperature (1400 rpm; 25% load; 17.5 CR).

Figure 20: Effect of compression ratio on in-cylinder pressure (1400 rpm; 50% load; 0% EGR).

Nomenclature

U:	State vector
F:	Flux vector
S:	Source term in the pipe flow equation
S_A:	Source caused by axial changes in pipe flow
S_R:	Source caused by homogeneous chemical reactions, heat, and mass transfer terms between the gas and solid phase in pipe flow
m_c:	Mass in the cylinder
u:	Specific internal energy
p_c:	Cylinder pressure
V:	Cylinder volume
Q_F:	Fuel energy
Q_w:	Wall heat loss
α:	Crank angle
h_{BB}:	Enthalpy of blow-by
$(dm_{BB})/d\alpha$:	Blow-by mass flow
dm_i:	Mass element flowing into the cylinder
dm_e:	Mass element flowing out of the cylinder
h_i:	Enthalpy of the in-flowing mass
h_e:	Enthalpy of the mass leaving the cylinder
q_{ev}:	Evaporation heat of the fuel
f:	Fraction of evaporation heat from the cylinder charge
m_{ev}:	Mass of evaporating fuel
nSpcGas:	Number of species in the gas phase
MW_i:	Species molecular weight
u_i:	Species internal energy
w_i:	Species mass fraction
ρ:	Mixture density
$\dot{\omega}_i$:	Species reaction rate
C:	Compression ratio
R:	Ratio of the crank radius to the length of the connecting rod.

Acknowledgment

References

[1] M. Yao, Z. Zheng, and H. Liu, "Progress and recent trends in homogeneous charge compression ignition (HCCI) engines," *Progress in Energy and Combustion Science*, vol. 35, no. 5, pp. 398–437, 2009.

[2] N. P. Komninos, D. T. Hountalas, and D. A. Kouremenos, "Description of in-cylinder combustion processes in HCCI engines using a multi-zone model," SAE Paper 2005-01-0171, 2005.

[3] S. B. Fiveland and D. N. Assanis, "A four-stroke homogeneous charge compression ignition engine simulation for combustion and performance studies," SAE Paper 2000-01-0332, 2000.

[4] Z. Wang, S. J. Shuai, J. X. Wang, and G. H. Tian, "Modelling of HCCI combustion: from 0D to 3D," SAE Paper 2006-01-1364, 2000.

[5] T. W. Ryan III and T. J. Callahan, "Homogeneous charge compression ignition of diesel fuel," SAE Paper 961169, 1996.

[6] G. B. Raya, "Chemical kinetic mechanism reduction, multizone and 3D-CRFD modelling of homogeneous charge compression ignition engines," Dissertation ETH 16437, Swiss Federal Institute of Technology, Zurich, Switzerland, 2006.

[7] AVL Boost v10 Theory Manual.

[8] AVL Boost v10 Users Guide.

[9] FIRE v9.1 CFD Solver Help Manual.

[10] A. Bourdon, G. Rymer, and R. Wanker, "Optimization of a 5-step kinetic scheme for HCCI applications," SAE Paper 2004-01-0559, 2006.

[11] T. Lovas, F. Mauss, N. Peters, and C. Hasse, "Modeling of HCCI combustion using adaptive chemical kinetics," SAE Paper 2002-01-0426, 2002.

[12] P. Maigaard, F. Mauss, and M. Kraft, "Homogeneous charge compression ignition engine: a simulation study on the effects of inhomogeneities," Paper 2000-ICE-275, ICE-Vol. 34-2, ASME, 2000.

[13] AVL Concerto v3.9 Help Manual.

[14] M. Noguchi, Y. Tanaka, T. Tanaka, and Y. Takeuchi, "A study on gasoline engine combustion by observation of intermediate reactive products during combustion," SAE Paper 790840, 1979.